Conserving relativistic many-body approach: Equation of state, spectral function, and occupation probabilities of nuclear matter

Fred de Jong and Rudi Malfliet
Kernfysisch Versneller Instituut, 9747 AA Groningen, The Netherlands
(Received 7 January 1991)

Starting from a relativistic Lagrangian we derive a "conserving" approximation for the description of nuclear matter. We show this to be a nontrivial extension over the relativistic Dirac-Brueckner scheme. The saturation point of the equation of state calculated agrees very well with the empirical saturation point. The conserving character of the approach is tested by means of the Hugenholtz–van Hove theorem. We find the theorem fulfilled very well around saturation. A new value for compression modulus is derived, $K = 310$ MeV. Also we calculate the occupation probabilities at normal nuclear matter densities by means of the spectral function. The average depletion κ of the Fermi sea is found to be $\kappa \sim 0.11$.

I. INTRODUCTION

The theoretical microscopic description of nuclear matter is a long-standing problem. The relative simple structure of the system, as compared to finite nuclei, allows one to focus especially on the differences between the various schemes proposed to calculate the properties of the system. Quantities like binding energy, saturation density, compression modulus, momentum distribution, and single-particle potential are typical examples of such observables. The complexity and strength of the nuclear interaction render a simple perturbation expansion useless and ask for a more sophisticated approach.

One can distinguish between phenomenological approaches and microscopical models. In a phenomenological approach, like, e.g., the σ-ω model of Serot and Walecka [1], one constructs an effective theoretical framework for the description of the many-body system. The free parameters are fixed by reproducing some of the known empirical properties, in the case of the σ-ω model the empirical saturation point. One is then able to predict the binding energy for all densities and, e.g., also the compression modulus. The latter quantity is not in very good agreement with known values and demonstrates the weakness of this approach.

Microscopic models are more ambitious in their aims. One starts with a "realistic" interaction, i.e., an interaction that reproduces the known nucleon-nucleon interaction data like phase shifts and the deuteron properties. By the use of a well-defined many-body scheme, the properties of the nuclear matter system are calculated. Then the comparison with the empirical data will decide whether the model is succesfull or not. However, the interaction, although fairly well known, cannot be determined uniquely, neither is the many-body scheme unique. Since the results are an interplay of the scheme and interaction employed, it is impossible to discriminate between the interaction or the scheme being wrong in the case the model fails to describe the empirical data. The most sensible approach is to calculate many physical observables within the same model. Also one should try and place the model on a firm theoretical basis: It should be clear what the physical implications of the approximations involved are. Then the model can be judged by evaluating the severeness of the approximations involved and by comparing the whole set of calculated observables with the data. A succesfull description of the saturation properties can only provide a motivation for a calculation of other observables.

At present two main approaches are used. On one hand, the variational approach pioneered and pursued by Fantoni and Pandharipande [2]. On the other hand, the Brueckner/Green's-function approaches, e.g., used by the Liège group [3] and the Bonn group [4]. The Brueckner scheme can be related to the Green's-functions approach by the hole-line expansion [3, 5] and turns out to be the first order in the hole-line expansion. The hole-line expansion provides a tool for a systematic study of the validity of the Brueckner scheme.

The failure of the (nonrelativistic) Brueckner-type calculations to reproduce the empirical saturation point has focused nuclear matter calculations on this very point. The saturation points obtained using various potentials form a "Coester band" [6], the position on the band depends on the strenght of the tensor force of the interaction used. Inclusion of higher-order diagrams showed no significant improvement [7]. This led to the conclusion that it was impossible to reproduce the empirical saturation point in nonrelativistic Brueckner theory without the inclusion of genuine three-body forces. Incorporation of relativistic effects into the Brueckner scheme, first pursued by Celenza *et al.* [8] later followed by other groups [4, 9, 10], did give an improvement. The relativistic Brueckner Hartree-Fock model gave a saturation point and compressibility compatible with the data. The relativistic aspects included were (a) the proper kinematical factors, (b) the explicit Lorentz structure of the self-energy, and (c) the use of "effective" spinors. This ap-

parent success is the motivation for the calculation of other nuclear matter observables. It also prompted us to investigate further the theoretical basis of the model. As we demonstrate later on, the latter will lead to the conclusion that one has to go to all orders in the hole-line expansion to preserve important and very general properties of the system.

Only in more recent years results of other nuclear matter properties calculated within the nonrelativistic Brueckner scheme, like the nucleon momentum distribution [11–13], have become available. Recently first investigations within the Green's-function approach into the nuclear spectral function were carried out [14]. Also the variational results on this subject are of a recent date [2, 15]. Within the relativistic Brueckner scheme no results are available yet, apart from the estimate by Jaminon and Mahaux [16] of the occupation probabilities. The present work includes a full calculation of the momentum distribution by means of the spectral function.

In this paper we will subject our relativistic many-body model to an additional constraint, namely, that the model should be conserving [17]; i.e., the extension of the many-body scheme to a nonequilibrium situation should conserve, e.g., total energy, momentum, and particle number. The next section is devoted to a derivation of the model from first principles. We will propose a prescription that is conserving and contains the Brueckner scheme. It will turn out, however, that the approach is equivalent to going to all orders in the hole-line expansion. The first part of the third section contains results on the equation of state and related quantities. In the second part of the third section we will calculate a relativistic spectral function and obtain with this the momentum distribution in nuclear matter at saturation. The last section is a summary of the results.

II. FORMALISM

The following subsections are a brief overview of the underlying formalism of our calculations. For a thorough account of the material presented in sections A and B we refer to Ref. [18].

A. Preliminaries

Our starting point is a relativistic Lagrangian containing nucleons and mesons. The nucleons are treated as pointlike particles so form factors need to be introduced to cut off the short distance behavior of the interaction. The free parameters of the Lagrangian are fitted to N-N scattering data [9]. This was achieved by solving the three-dimensional (Thompson) reduction of the Bethe-Salpeter equation using a one-boson-exchange interaction corresponding to our initial Lagrangian. The Euler-Lagrange equations of this system are a coupled set of equations for both the nucleon and meson fields. By inverting the meson fields one can eliminate these, thereby introducing an interaction V_{12} of the one-boson-exchange type.

In this paper we will discuss results for nuclear matter in equilibrium based on an approximation which respects causality, analyticity, conservation laws, and general thermodynamic relations. It will be constructed as the (static) equilibrium limit of a more general (kinetic) nonequilibrium theory. The latter will be obtained through the so-called T-matrix approximation. This approximation is very reminiscent of the three-dimensional Bethe-Salpeter treatment mentioned above, and it coincides with it at zero baryon density. The general (time-dependent) nonequilibrium framework (which is reviewed in Ref. [18]) will allow us to specifically check whether the approximation used does not violate any of the aforementioned principles. The approximation discussed here (the T-matrix approximation) is but one example of a particular truncation in the hierarchy of Green's functions which describe the N-body dynamics. Therefore it falls into the category of kinetic theories. Such a kinetic theory will obey the second law of thermodynamics; i.e., the change in entropy is always positive. This implies that the time development of the many-body system as described by the kinetic theory has a specific direction in time. This in contrast to the Lagrangian which is invariant under time reversal. So somewhere in the derivation of the kinetic theory the time-reversal invariance is removed. Consequently, we have to treat carefully the dependence of the nucleon field operators on the temporal development of the system to incorporate this in a proper way.

An elegant and transparent way of dealing with this problem is defining a Keldysh contour [19]: a time path running from $-\infty$ to ∞ and then backwards from ∞ to $-\infty$ (Fig. 1). The algebra on the contour has a simple matrix structure and keeps track of the time dependences in a transparant way. When a field develops chronologically in time it is on the upper branch, when it develops achronologically in time it is on the lower branch of the contour. On the contour we define an ordering P such that a field operator which is "later" on the contour is put to the left of earlier ones, including the appropiate sign changes associated with the (anti)commutation relations of the fields. This order operator enables us to define the path-ordered n-body Green's function [a 1 denotes the coordinates in space time $(t_1, \bar{x}_1)$, conventionally $\bar{\psi} = \psi^\dagger \gamma^0$]

$$\mathbf{G}(1...n, 1'...n') = (-i)^n \langle P\left[\psi(1)\cdots\psi(n)\bar{\psi}(n')\cdots\bar{\psi}(1')\right]\rangle. \tag{1}$$

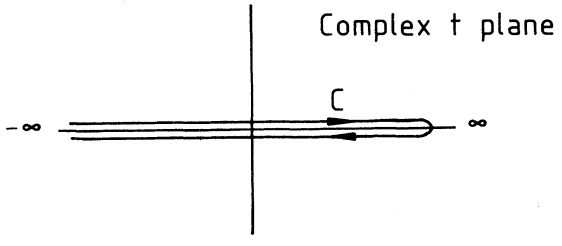

FIG. 1. The Keldysh time contour.

Due to the nucleon field equations these n-body Green's functions form a Martin-Schwinger hierarchy of equations, linking lower-order Green's functions to higher-order ones. The purpose now is to truncate this hierarchy at a certain level in such a way that the resulting transport equation still obeys the conservation laws appropiate to the many-body system; i.e., the approximative equations governing the system should conserve quantities like total number, energy, and total momentum. The criteria for such a "conserving" approximation were first developed by Baym and Kadanoff [17].

To connect the path-ordered Green's functions to the conventional ones let us consider the one-body Green's function. The two fields have four distinct relative positions on the time contour and can be ordered in a 2×2 matrix (such a matrix is indicated by a bold capital; a "+" denotes a time on the upper branch, a "−" a time on the lower branch):

$$\mathbf{G}(1,1') = \begin{pmatrix} G_{++}(1,1') & G_{+-}(1,1') \\ G_{-+}(1,1') & G_{--}(1,1') \end{pmatrix} = \begin{pmatrix} G^c(1,1') & G^<(1,1') \\ G^>(1,1') & G^a(1,1') \end{pmatrix}, \tag{2}$$

with

$$\begin{aligned} G^c(1,1') &= -i\langle T\left[\psi(1)\bar{\psi}(1')\right]\rangle, \\ G^a(1,1') &= -i\langle \tilde{T}\left[\psi(1)\bar{\psi}(1')\right]\rangle, \\ G^<(1,1') &= i\langle\bar{\psi}(1')\psi(1)\rangle, \\ G^>(1,1') &= -i\langle\psi(1)\bar{\psi}(1')\rangle. \end{aligned} \tag{3}$$

T and $\tilde{T}$ are the chronological and antichronological time-ordering operators, respectively. The Green's functions we defined are the causal, acausal, and the two correlation Green's functions, as can be found in, e.g., Ref. [20]. With these we can define the retarded and advanced Green's functions, which will turn out to be the most convenient ones to use later:

$$\begin{aligned} G^{(+)}(1,1') &= G^c(1,1') - G^<(1,1') \\ &= \theta(t_1 - t_{1'})[G^>(1,1') - G^<(1,1')], \end{aligned} \tag{4}$$

$$\begin{aligned} G^{(-)}(1,1') &= G^c(1,1') - G^>(1,1') \\ &= -\theta(t_{1'} - t_1)[G^>(1,1') - G^<(1,1')]. \end{aligned}$$

Only two of the total set of different Green's functions are independent, so we only need two Green's functions (or combinations) to describe the system completely. A particular important combination of two Green's functions is the spectral function

$$A(1,1') = i(G^{(+)} - G^{(-)}) = i(G^> - G^<) = \{\bar{\psi}(1'), \psi(1)\}, \tag{5}$$

where $\{\,,\,\}$ is the anticommutator. Letting t_1 approach $t_{1'}$ we obtain the equal-time anticommutator of the fields, and we have the property

$$\lim_{t_1 \to t_{1'}} A(1,1') = \gamma^0\,\delta^3(x_1 - x_{1'}). \tag{6}$$

In momentum space this relation takes the form of a sum rule, which we will encounter later on.

Let us now examine the Martin-Schwinger hierarchy as defined on the contour. Its first equation, linking $\mathbf{G}_1$ to $\mathbf{G}_{12}$, is given by

$$\begin{aligned} &D(1,1''')\mathbf{G}_1(1''',1') \\ &\quad = \underline{\delta}(1-1') - i\langle 1\,2|\mathbf{V}_{12}|1''2''\rangle\mathbf{G}_{12}(1''2'',1'2^+). \end{aligned} \tag{7}$$

The indices $1'', 1''', 2$, and $2''$ are summed and integrated over. For the 2 variable this amounts to a trace. $D(1,1''')$ is the differential operator associated with the Dirac equation, $\underline{\delta}$ is the δ function generalized on the contour [18]. $\mathbf{V}_{12}$ is the one-boson-exchange interaction on the contour [18], 2^+ indicates a time infinitesimally later on the contour than 2. The self-energy (mass operator) $\mathbf{\Sigma}$ has the same time structure as $\mathbf{G}_1$, its components are put in a 2×2 matrix in the same way as $\mathbf{G}_1$. Equation (7) suggests the definition

$$\mathbf{\Sigma}(1,1''')\mathbf{G}(1''',1') = -i\langle 1\,2|\mathbf{V}_{12}|1''2''\rangle\mathbf{G}(1''2'',1'2^+). \tag{8}$$

Again the indices $1'', 1''', 2$, and $2''$ are integrated and summed over. Inserting this definition into Eq. (7) leads to the Dyson equation for the one-body Green's function (again in matrix form, suppressing the indices)

$$\mathbf{G} = \mathbf{G}_0 + \mathbf{G}_0\mathbf{\Sigma}\mathbf{G}, \tag{9}$$

where $\mathbf{G}_0$ is the noninteracting one-body Green's function, the solution of Eq. (7) with $\mathbf{V}_{12}$ set to zero.

B. Truncation of the hierarchy

From the above it follows that an ansatz for $\mathbf{G}_{12}$ determines $\mathbf{\Sigma}$ and consequently $\mathbf{G}_1$. When expressing $\mathbf{G}_{12}$ in the one-body Green's functions, the Martin-Schwinger hierarchy is truncated. To be consistent it has also to fulfill the requirements for a conserving approximation as given by Baym and Kadanoff [17]. These imply keeping the proper symmetries for $\mathbf{G}$ and using the approximated "dressed" Green's function in all expressions; i.e., one has to solve the emerging equations self-consistently. Besides, the specific ansatz should respect the particular time behavior of the equations and the quantities which obey these equations. For instance from Eq. (9) one can deduce Dyson equations for the retarded, advanced, causal, and acausal Green's functions. However, the proposed ansatz for $\mathbf{\Sigma}$ might violate these time-ordering properties which in general are guaranteed in the theory. As a consequence, if one affects these properties one will destroy important relations such as dispersion relations that follow directly from the retarded or advanced time behavior in the Fourier-transformed space.

In the particular ansatz the physical properties of the system under consideration have to be reflected. When three-body forces are present one certainly has to incorporate $\mathbf{G}_{123}$ in the ansatz for $\mathbf{G}_{12}$. In our model we have a two-body interaction and we will restrict ourselves to expressing $\mathbf{G}_{12}$ in $\mathbf{V}_{12}$ and $\mathbf{G}_1$. The simplest choice is taking for $\mathbf{G}_{12}$ the antisymmetrized direct product of two one-body Green's functions, then we obtain the Hartree-

Fock expressions for the self-energy. However, the resulting transport equation does not contain a collision term and thus will not be able to describe nuclear matter in nonequilibrium.

Also the range of the interaction has to be considered in the particular ansatz. A long-range interaction, like the one in the electron gas, has to be treated with a truncation scheme that has the characteristics of the random-phase-approximation approach. In the case of the nucleon-nucleon interaction short-range correlations induced by the hard core are most important. This consideration led to the classical Brueckner scheme of summing all ladder diagrams to "soften" the hard core of the interaction. A conserving ladder-type approximation is the T-matrix approximation. As we will see later on this approximation is an extension over the conventional Brueckner scheme; see Ref. [18] for an extensive discussion. The T matrix is defined by

$$\langle 12|\mathbf{T}_{12}|1'2'\rangle = \langle 12|\mathbf{V}_{12}|1'2'\rangle + i\langle 12|\mathbf{V}_{12}|1''2''\rangle \mathbf{G}_1(1'',1''')\mathbf{G}_2(2'',2''')\langle 1'''2'''|\mathbf{T}_{12}|1'2'\rangle, \tag{10}$$

where the indices $1'', 1''', 2''$, and $2'''$ are integrated and summed over. From this definition we find a relation between $\mathbf{G}_{12}$ and $\mathbf{G}_1$, upon inserting this in Eq. (8) we find for the self-energy

$$\mathbf{\Sigma}_1(1,1') = -i\langle 12|\mathbf{T}_{12}|1'2'\rangle \mathbf{G}_2(2',2^+). \tag{11}$$

Again the indices 2 and $2'$ are integrated and summed over. So by making the T-matrix approximation we have defined all the necessary quantities in terms of the one-body Green's function. The theory consists of a set of coupled equations, Eqs. (9), (10), and (11), in 2×2 "Keldysh space," that has to be solved self-consistently. When we write out the matrix content of the equations explicitly in terms of causal, acausal, and correlation components we end up with a set of complicated equations. Only when we take the retarded and advanced components we have formally a simple set of equations:

$$\begin{aligned} g^{(\pm)} &= g_0^{(\pm)} + g_0^{(\pm)}\Sigma^{(\pm)}g^{(\pm)}, \\ \Sigma^{(\pm)} &= -i(T_{12}^{(\pm)}g_2^< + T_{12}^<g_2^{(\mp)}), \\ T_{12}^{(\pm)} &= V_{12} + iV_{12}(g_1g_2)^{(\pm)}T_{12}^{(\pm)}, \\ T_{12}^< &= iT_{12}^{(+)}g_1^<g_2^<T_{12}^{(-)}. \end{aligned} \tag{12}$$

The specific form of the propagators $g^{(\pm)}$, $g^<$, $g^>$, and $(g_1g_2)^{(\pm)}$ will be given below. The full set Eq. (12) corresponds to a conserving approximation. Any additional simplification may affect the proper time structure and will destroy this important property. As we will discuss later on, the conventional Brueckner scheme, which is such a simplification, is not conserving.

In this set of equations contributions of negative-energy states are still present. A proper treatment of these would mean a renormalization scheme within the T-matrix approximation. To our knowledge such a renormalization scheme within the T-matrix approximation has, up to now, not been proposed. While there are physical arguments why to use the T-matrix approximation when including only positive-energy states, it is questionable whether the T-matrix approximation provides the most important diagrams when one does include negative-energy states. So we will take a pragmatic viewpoint and omit the negative-energy states, taking $\Sigma^{(+)} = 0$ in the vacuum. By fitting the scattering matrix $T^{(+)}$ to N-N scattering data we can assign to the coupling constants and meson masses their physical values; this fixes all free parameters in the Lagrangian. The results of this fit are given in Ref. [9]. The fit provides us with the one-boson-exchange interaction used in the calculations presented in the next sections. So by giving the parameters in the Lagrangian their physical values we have renormalized our theory "effectively." In other words, one eliminates (through a projection) the contribution of negative-energy states in the vacuum (no medium, only the bare nucleon-nucleon system) and treats the resulting equations of motion as an effective theory. This approximation induces problems when "switching on" the medium. It seems natural in this case to restrict ourselves still to a projection on *bare* postive-energy states. However, in order to obtain a conserving approach this procedure is deficient, as can be seen by inspecting the requirements for a conserving approach, which rely strongly on self-consistency. Our prescription therefore is to project on positive-energy *effective* spinors. While these are a mixture of *bare* positive- and negative-energy spinors they guarantee the conserving character of the model. In the no-medium limit this leads to the proper starting point, i.e., bare positive-energy spinors.

Our philosophy is the following: We first define our approximation in the most general scheme (nonequilibrium, relativistic) and constrain it such that important physical laws are not violated. Using this as our basic ansatz we then simply construct the appropiate limits (equilibrium, nonrelativistic). Going the other way has the danger that one sums in equilibrium certain diagrams which correspond to a nonconserving counterpart in nonequilibrium.

C. Relativistic aspects

To examine the content of the set of equations (12) further we now specify the propagators. In the case of nuclear matter it is convenient to Fourier transform to four-momentum space. For the noninteracting propagators we find the following expressions:

$$\begin{aligned} g_0^<(p) &= 2\pi i\frac{m}{E_p}[\,\delta(p_0 - E_p)\theta(p_f - |\bar{p}|)\Lambda^+(p) \\ &\qquad -\delta(p_0 + E_p)\Lambda^-(p)], \\ g_0^>(p) &= -2\pi i\frac{m}{E_p}\delta(p_0 - E_p)\theta(|\bar{p}| - p_f)\Lambda^+(p), \\ g_0^{(\pm)}(p) &= \frac{\not{p} + m}{p^2 - m^2 \pm i\epsilon} \pm 2\pi i\frac{m}{E_p}\delta(p_0 + E_p)\Lambda^-(p). \end{aligned} \tag{13}$$

With p the four-vector $(p_0,\vec{p})$, the single-particle energy $E_p = \sqrt{p^2+m^2}$, p_f is the Fermi momentum, and $\Lambda^{\pm}(p)$ are the usual positive- and negative-energy projection operators.

The self-energy $\Sigma^{(+)}$ can be decomposed in Lorentz components, in nuclear matter only the scalar and vector components are nonzero [21]:

$$\Sigma^{(+)}(p) = \Sigma_s^{(+)}(p) - \gamma^0\Sigma_0^{(+)}(p) + \vec{\gamma}\cdot\vec{p}\Sigma_v^{(+)}(p). \tag{14}$$

Inserting this in the Dyson equation for $g^{(+)}$ suggests the following definitions for "effective" quantities:

$$\begin{aligned} m^* &= m + \mathrm{Re}[\Sigma_s^{(+)}(p)],\\ p_0^* &= p_0 + \mathrm{Re}[\Sigma_0^{(+)}(p)],\\ \vec{p}^{\,*} &= \vec{p}\{1 + \mathrm{Re}[\Sigma_v^{(+)}(p)]\}. \end{aligned} \tag{15}$$

Re denotes the real part; note that the effective quantities are energy and momentum dependent. These definitions allow us to solve the Dyson equation formally as

$$g^{(+)} = \frac{1}{\not{p}^* - m^* - i\mathrm{Im}(\Sigma^{(+)}) + i\epsilon}. \tag{16}$$

The full propagator is associated with an effective ("dressed") spinor, denoted by $u^*(\vec{p})$. The asterisk indicates the effective character and should not be confused with complex conjugation. The *effective* spinor, which we will use extensively, is defined as the on-shell positive-energy solution of the "dressed" Dirac equation with the imaginary part of $\Sigma^{(+)}$ set to zero.

$$u_r^*(\vec{p}) = \left(\frac{E_p^*+m^*}{2m^*}\right)^{\frac{1}{2}}\begin{pmatrix}1\\ \dfrac{\vec{\sigma}\cdot\vec{p}^{\,*}}{E_p^*+m^*}\end{pmatrix}\chi_r, \tag{17}$$

χ_r is the state vector in spin space. The effective spinors are normalized according to $\bar{u}_r^*(\vec{p})\,u_s^*(\vec{p}) = \delta_{rs}$.

By using the definitions for $g_0^>$ and $g_0^<$ we find that in the noninteracting system the spectral function $a(p)$ is a δ function of the energy. We project on positive- (negative-) energy states by taking the spectral function between positive- (negative-) energy spinors, respectively. A more general treatment of the spectral function including negative-energy states can be found in Ref. [22]. In the noninteracting case we have

$$\begin{aligned} \bar{u}(\vec{p})\,a_0(p)\,u(\vec{p}) &= 2\pi\frac{m}{E_p}\delta(p_0 - E_p),\\ \bar{v}(\vec{p})\,a_0(p)\,v(\vec{p}) &= 2\pi\frac{m}{E_p}\delta(p_0 + E_p). \end{aligned} \tag{18}$$

In the case of an interacting system we have to isolate the positive-energy part of the spectral function. To do so we start with the defining equation of $g^{(+)}$

$$\begin{aligned} &(\not{p} - m - \Sigma^+)\,g^{(+)}(p) = 1 \;\Leftrightarrow\\ &(\not{p} - m - \Sigma^+)(\Lambda^{+^*} + \Lambda^{-^*})g^{(+)}(p) = (\Lambda^{+^*} + \Lambda^{-^*}). \end{aligned} \tag{19}$$

Now, in our case, $\Lambda^{-^*}\,\Sigma^{(+)} = 0$ and $\Lambda^{+^*}\,\Sigma^{(+)} = \Sigma^{(+)}$; i.e., we project on *effective* positive-energy states. Using the definition $\Lambda^{+^*} \equiv u^*(p)\otimes\bar{u}^*(p)$, we obtain for the positive-energy part of $g^{(+)}$

$$\bar{u}^*(\vec{p})g^{(+)}(p)u^*(\vec{p}) = \frac{m^*}{E_p^*}\left[p_0^* - E_p^* + i\mathrm{Im}\left(\Sigma_0^{(+)} - \frac{m^*}{E_p^*}\Sigma_s^{(+)} - \frac{p^*}{E_p^*}p\Sigma_v^{(+)}\right)\right]^{-1}. \tag{20}$$

The positive-energy-projected spectral function is now found to be

$$\bar{u}^*(\vec{p})a(p)u^*(\vec{p}) = \frac{m^*}{E_p^*}\frac{2\mathrm{Im}[\Sigma_0^{(+)} - (m^*/E_p^*)\Sigma_s^{(+)} - (p^*/E_p^*)p\Sigma_v^{(+)}]}{(p_0^* - E_p^*)^2 + \mathrm{Im}[\Sigma_0^{(+)} - (m^*/E_p^*)\Sigma_s^{(+)} - (p^*/E_p^*)p\Sigma_v^{(+)}]^2}. \tag{21}$$

This form has a straightforward nonrelativistic limit and can be compared to the nonrelativistic spectral function [14, 18].

In momentum space the property Eq. (6) has the form of a sum rule. Taking the Fourier transform of Eq. (6) between positive and negative effective spinors we obtain the sum rule for the positive- and negative-energy-projected spectral functions separately

$$\begin{aligned} &\int\frac{dp_0}{2\pi}\frac{E_p^*}{m^*}\bar{u}^*(\vec{p})a(p)u^*(\vec{p})\\ &\qquad = \int\frac{dp_0}{2\pi}\frac{E_p^*}{m^*}\bar{v}^*(\vec{p})a(p)v^*(\vec{p}) = 1. \end{aligned} \tag{22}$$

Note that the normalization factor E_p^*/m^* cancels the factor m^*/E_p^* encountered in the spectral function Eq. (21). In the following we incorporate this normalization factor into $a(p)$ by defining

$$\tilde{a}(p) = \frac{E_p^*}{m^*}\bar{u}^*(\vec{p})a(p)u^*(\vec{p}). \tag{23}$$

When the imaginary part is small compared with the real part we are allowed to take the "quasiparticle" approximation, i.e., neglect the imaginary part as compared to the real part. The spectral function then becomes a δ function but now of the "effective" mass and momenta

$$\tilde{a}(p) = 2\pi\delta(p_0^* - E_p^*). \tag{24}$$

The sum rule Eq. (22) is fulfilled since setting the imaginary part of the retarded and advanced Green's functions equal to zero implies that the real part does not depend on p_0. This is because the real part and imaginary part are related by a dispersion relation. Equation (24) defines the single-particle energy of the "quasiparticle"

$$\epsilon_{\mathrm{sp}}^* = \sqrt{|\vec{p}^{\,*}|^2 + m^{*2}} - \Sigma_0^{(+)} = E_p^* - \Sigma_0^{(+)}. \tag{25}$$

Note that the common practice in conventional Brueckner calculations of fixing the values of the self-energies to the value at the Fermi surface [9, 10] is consistent with taking the quasiparticle approximation, since the imaginary part of the self-energy is rigorously zero at the Fermi surface [23].

As can be seen from Eq. (12) all the appearing T matrices can be expressed in terms of $T^{(+)}$ ($T^{(-)}$ is the conjugate of $T^{(+)}$). In the definition of $T^{(+)}$ we encounter the term $(g_1 g_2)^{(+)}$ which can be worked out to give [18]

$$(g_1 g_2)^{(+)}(p) = i \int \frac{dp_0' dp_0''}{(2\pi)^2} \frac{g_1^{>}(p') g_2^{>}(p'') - g_1^{<}(p') g_2^{<}(p'')}{p_0 - p_0' - p_0'' + i\epsilon}. \tag{26}$$

Since $g^{<}$ scales with $n(p)$, the particle momentum distribution, and $g^{>}$ scales with $1 - n(p)$ we see that $T^{(+)}$ contains both propagation of particle-particle and hole-hole states. Another feature is that $T^{(+)}$ is analytic in the upper half of the complex p_0 plane. In order to reduce the set of equations (12), corresponding to the T-matrix approximation, to the conventional Brueckner model (termed Dirac-Brueckner in case of the relativistic version), we have to make three additional approximations that lead to a nonconserving truncation of hierarchy. First, we have to neglect the hole-hole propagating term in $T^{(+)}$. Second (and a consequence of the first approximation), we have to neglect the second term in the definition of $\Sigma^{(+)}$ in Eq. (12). The third approximation is to use the quasiparticle approximation. Results for nuclear matter using these approximations have been presented in Ref. [9]. In the following these will be referred to as Dirac-Brueckner. The conserving approach corresponding to Eq. (12) will be called the T-matrix approximation. In the next section we will present new results based on the T-matrix approximation. We do incorporate the hole-hole propagation, i.e., do not make the first two approximations mentioned above.

However, we still invoke the quasiparticle approximation. By doing so we neglect the imaginary part of the self-energy. This also implies that the real part of the self-energy is constant as a function of the energy p_0 because the real and imaginary parts of the self-energy are related by a dispersion relation. Since the self-energy does acquire an imaginary part in the quasiparticle approximation, this approximation reduces the degree of self-consistency with which we solve Eq. (12). As long as the imaginary part of the self-energy is small compared to the real part, the deviations of the solution of Eq. (12) found when invoking the quasiparticle approximation from the fully self-consistent solution will be small.

Also, the method of projecting on effective positive-energy states relies on the imaginary part of the self-energy being small. In addition, the use of the quasiparticle approximation can be justified by the argument that the physical behavior of the system will mainly be determined by the particles close to the Fermi surface. At the Fermi surface the imaginary part of the self-energy is zero and the Fermi surface consists of quasiparticles with an infinite lifetime. So the quasiparticle approximation seems to be a reasonable starting point for a description of the system.

III. RESULTS

In this section we present results based on the T-matrix approximation. The first subsection deals with the properties of the equation of state calculated in the T-matrix approximation. In the second subsection we will deal with the energy (p_0) dependence of the self-energy and calculate the spectral function and occupation probabilities at normal nuclear matter density.

A. Equation-of-state of nuclear matter

In the practical solution of the set Eq. (12) we approximate the self-energies by their value on the Fermi surface. This is justified by the weak momentum dependence of the self-energies [9, 24]. Also the self-energy at the Fermi surface has a zero imaginary part, consequently the spectral function is a δ function so this choice is consistent with the quasiparticle approximation. An additional approximation is to set $\bar{p}^* = \bar{p}$, now $\Sigma_v^{(+)}$ has to be included in the effective mass [9, 10]

$$m_{sc}^* = \frac{m + \Sigma_s^{(+)}(p_f)}{1 + \Sigma_v^{(+)}(p_f)}. \tag{27}$$

This redefinition of m^* is needed in order that the effective spinor, Eq. (17), remains a solution of the "dressed" Dirac equation. Where there might be confusion about which effective mass is used we will refer to the definition Eq. (27) as the "self-consistent" effective mass. The virtue of this approach is that the self-consistent effective mass is the only independent self-consistent iteration parameter in the set Eq. (12). The eigenvalue of the Dirac equation is now

$$E_p^* = \sqrt{|\bar{p}|^2 + m_{sc}^{*2}}. \tag{28}$$

We now discuss the calculation of the $T^{(+)}$ matrix. The $T^{(+)}$ matrix is most easily evaluated in the two-particle center-of-mass frame (for a more detailed account we refer to Ref. [9]). In this frame the total effective four-momentum has the form $(\sqrt{s^*}, \bar{0})$. The transformation to this frame is uniquely defined by the set (s^*, P), where P is the total three-momentum in the nuclear matter rest frame. The dependence on the direction of P is removed by making the angle average approximation to the Pauli-blocking operator. The results are not sensitive to this averaging procedure [25]. Also a three-dimensional (Thompson) reduction of the Bethe-Salpeter T-matrix equation is performed, thereby removing retardation effects in $\mathbf{V}_{12}$. In the two-particle c.m. frame we then have to solve the following equation (suppressing spin indices):

$$\langle\bar{p}|T^{(+)}(s^*,P)|\bar{p}'\rangle = \langle\bar{p}|V|\bar{p}'\rangle + \int \frac{d\bar{p}''}{(2\pi)^3}\langle\bar{p}|V|\bar{p}''\rangle \frac{{m^*_{sc}}^2}{{E^*_{p''}}^2} \frac{\bar{Q}_p(p'',s^*,P)-\bar{Q}_h(p'',s^*,P)}{\sqrt{s^*}-2E^*_{p''}+i\epsilon}\langle\bar{p}''|T^{(+)}(s^*,P)|\bar{p}'\rangle. \quad (29)$$

$\bar{Q}_p(p'',s^*,P)$ is the relativistic angle-averaged Pauli-blocking operator [9], which is simply the angle average of $[1-n(\bar{p}'')][1-n(-\bar{p}'')]$. The momentum distribution $n(\bar{p})$ equals, at zero temperature, $\theta(p_f-|\bar{p}|)$. The dependence on (s^*,P) is due to the operator being evaluated in the two-particle c.m. frame, where the Fermi sea is deformed because of the Lorentz transformation defined by (s^*,P). $\bar{Q}_h(p'',s^*,P)$ is the angle average of $n(\bar{p}'')n(-\bar{p}'')$; it has a similar structure as $\bar{Q}_p$ and is responsible for the hole-hole propagation. For on-shell scattering we have $p'=p$ and $\sqrt{s^*}=2E^*_p$. We solve Eq. (29) in full momentum-spin space, and thus we do not use a partial-wave representation. For more details we refer to Ref. [9]. After obtaining a solution for $T^{(+)}$ we are in the position to calculate the first term in the expression for $\Sigma^{(+)}$, Eq. (12), formally written as $-iT^{(+)}g^<$. We transform the integration to the c.m. coordinates s^* and P. This gives

$$-iT^{(+)}g^<(p_f) = \int_0^{4p_f^2} dP^2 \int_{s^*_{\min}}^{s^*_{\max}} ds^* \frac{1}{32p_f\pi^2}\frac{1}{E^*_{p_f}+E^*_q}\mathrm{Tr}\left[(\not{q}^*+m^*_{sc})\langle p|T^{(+)}(s^*,P)|p\rangle_{\mathcal{A}}\right]. \quad (30)$$

The symbol $\mathcal{A}$ denotes antisymmetrization, Tr taking the trace over the spin-isospin space; $s^*=2E^*_p$, q is the momentum of the integrated particle in the nuclear matter rest frame, found by applying the inverse transformation to (s^*,P). Also $s^*_{\min}=(E^*_{p_f}+E^*_{q_{\min}})^2-P^2$, with $q_{\min}=|P-p_f|$ and $s^*_{\max}={4E^*_{p_f}}^2-P^2$. Apart from the hole-hole propagation in $T^{(+)}$ this contribution is the same as the Dirac-Brueckner self-energy [9]. In order to split the self-energy into its Lorentz components we project $T^{(+)}$ matrix on a basis of 5 Lorentz-invariant amplitudes, where we use the pseudovector instead of the pseudoscalar as proposed by Horowitz and Serot [10]. This choice is not unambiguous and can only be removed when one fully incorporates the negative-energy states [26]. The pseudovector and pseudoscalar amplitudes are equivalent on-shell, but they contribute differently to the Lorentz component of the self-energy. We prefer the use of the pseudovector for two reasons. First, the pion in our model has a pseudovector coupling. Second, the pseudovector coupling suppresses the coupling to negative-energy states as compared to the pseudoscalar choice. In both cases the Lorentz-invariant amplitudes are degenerate at zero angle. This we solve by projecting at two small finite angles $\theta^\epsilon_{1,2}$ and extrapolating to zero angle. As has been shown by Horowitz and Serot this limit exists [10]. The contribution of the amplitudes to the different Lorentz components of $\Sigma^{(+)}$ are then readily evaluated.

The second term in the definition of $\Sigma^{(+)}$ in Eq. (12), in formal notation $-iT^<g^{(-)}$, can be worked out in a similar fashion. We use the last equation of Eq. (12) to express $T^<$ in $T^{(\pm)}$. Again we need $T^<$ at finite scattering angles to project on Lorentz-invariant amplitudes, this is achieved by using the rotational properties of $T^{(\pm)}$. After evaluating all the δ functions and exploiting the kinematical restrictions of the $T^{(\pm)}$ matrices and intermediate states, we arrive at the following expression (again we transform to the appropiate c.m. coordinates s^*, P, and p):

$$-iT^<g^{(-)}(p_f) = -\int_0^{4p_f^2} dP^2 \int_{4m^{*2}_{sc}}^{4E^*_{p_f}-P^2} ds^* \int_{p_{\min}(s^*,P)}^{p_{\max}(s^*,P)} dp \frac{1}{(2\pi)^3}\frac{p'\,p\,s^*}{16p_f E^*_p (s^*+P^2)^{\frac{1}{2}}}$$
$$\times\mathrm{Tr}\left[\frac{1}{2E^*_q}\frac{(\not{q}^*+m^*_{sc})}{(s^*+P^2)^{\frac{1}{2}}-E^*_{p_f}-E^*_q-i\epsilon}\langle p,0,0|\tilde{T}^<(s^*,P)|p,\theta^\epsilon_{1,2},0\rangle_{\mathcal{A}}\right], \quad (31)$$

where $\tilde{T}^<$ is defined as

$$\langle p,0,0|\tilde{T}^<(s^*,P)|p,\theta^\epsilon_{1,2},0\rangle = \int\frac{d\Omega}{(2\pi)^2}\langle p,0,0|T^{(+)}(s^*,P)|p',\theta,\phi\rangle\bar{Q}_h(p',s^*,P)\langle p',\theta,\phi|T^{(-)}(s^*,P)|p,\theta^\epsilon_{1,2},0\rangle. \quad (32)$$

$\tilde{T}^<$ is related to $T^<$ by

$$\langle\bar{p}|T^<(s^*,P)|\bar{p}\rangle = \int_{4m^{*2}}^{4E^*_{p_f}-P^2} ds^*\,\langle\bar{p}|\tilde{T}^<(s^*,P)|\bar{p}\rangle, \quad (33)$$

where we used a notation in polar coordinates, $d\Omega$ is the integration over the polar angles. $\theta^\epsilon_{1,2}$ are the small angles needed for the projection, $\bar{Q}_h(p',s^*,P)$ is the same as Eq. (29). The intermediate state with momentum p' in $T^<$ is on shell, this is expressed by $p'=\sqrt{\frac{1}{4}s^*-{m^*_{sc}}^2}$. Again q is the momentum of the integrated particle in the nuclear matter rest frame, this is found by applying the inverse transform to p. The introduction of $\tilde{T}^<$ allowed us to interchange the integration ds^* and dp. It is then easy to incorporate the kinematical restrictions: P restricts s^* and the set (s^*,P) restricts p as is reflected in the

TABLE I. The self-consistent values at the Fermi surface, binding energy, and single-particle energy at the Fermi surface in the relativistic Dirac-Brueckner approach.

p_f (GeV/c)	m^* (GeV)	$\Sigma_s^{(+)}$ (GeV)	$\Sigma_0^{(+)}$ (GeV)	$\Sigma_v^{(+)}$ (−)	E_b (MeV)	$\epsilon_{sp}(p_f)$ (MeV)
0.21	0.719	−0.230	−0.177	−0.012	−11.3	−23.5
0.22	0.693	−0.258	−0.200	−0.016	−12.0	−24.2
0.23	0.667	−0.286	−0.224	−0.019	−12.6	−24.5
0.24	0.641	−0.314	−0.247	−0.024	−13.6	−25.0
0.25	0.614	−0.344	−0.272	−0.029	−14.2	−24.4
0.26	0.586	−0.375	−0.299	−0.035	−14.4	−22.5
0.27	0.555	−0.410	−0.330	−0.044	−14.7	−19.7
0.28	0.529	−0.435	−0.352	−0.045	−14.8	−15.5
0.29	0.510	−0.455	−0.372	−0.050	−14.0	−10.9
0.30	0.483	−0.490	−0.407	−0.068	−12.7	−3.0
0.32	0.424	−0.553	−0.477	−0.086	−8.6	22.2
0.34	0.371	−0.610	−0.554	−0.108	0.0	62.6
0.36	0.325	−0.659	−0.640	−0.134	14.3	119.8

integration limits. The integration limits $p_{\min}(s^*, P)$ and $p_{\max}(s^*, P)$ are given by the relations

$$E^*_{p_{\min}} = \frac{1}{\sqrt{s^*}}\left[(s^* + P^2)^{\frac{1}{2}} E^*_{p_f} - p_f P\right],$$
$$E^*_{p_{\max}} = \frac{1}{\sqrt{s^*}}\left[(s^* + P^2)^{\frac{1}{2}} E^*_{p_f} + p_f P\right]. \tag{34}$$

The contribution Eq. (31) to the self-energy has almost the same structure as the so-called "rearrangement" contribution [3], the difference being an additional factor $[1 - n(q)]$ that has to be put in the integrand of our expression, Eq. (31), to obtain the same functional form as the rearrangement contribution. And the contributions of the hole-hole propagation in $T^{(\pm)}$. From the presence of $\bar{Q}_h$ we infer that omitting hole-hole propagation in $T^{(+)}$ should be accompanied by omitting the $T^{<}g^{(-)}$ contribution to $\Sigma^{(+)}$. In principle, the denominator in Eq. (31) has a zero in the integration region. This we treated with a suitable subtraction method. The set of Eq. (12) can now be solved by iterating around the self-consistent effective mass. After evaluating the self-consistent effective mass we calculate the binding energy by its definition

$$E_b = \frac{1}{\rho}\int_0^{p_f} \frac{dp}{2\pi} p^2 \langle \bar{u}^*(p)|\gamma\cdot\bar{p} + m_N + \tfrac{1}{2}\Sigma^+|u^*(p)\rangle \times \frac{m^*_{sc}}{E^*_p} - m_N. \tag{35}$$

Results for a range of densities are given in Table II and presented in Fig. 2. For comparison we give in Table I the Dirac-Brueckner values. These are calculated using an improved computer code as compared to the one used for calculating our previous results [9]. The improvement included a more careful treatment [27] of the singularity in the T matrix encountered at certain densities [9]. Comparing with the Dirac-Brueckner results we see that around saturation the binding energy is lowered by $\sim$ 1 MeV. The saturation density is somewhat

TABLE II. The self-consistent values at the Fermi surface, binding energy, and single-particle energy at the Fermi surface calculated with a relativistic conserving approximation.

p_f (GeV/c)	m^* (GeV)	$\Sigma_s^{(+)}$ (GeV)	$\Sigma_0^{(+)}$ (GeV)	$\Sigma_v^{(+)}$ (−)	E_b (MeV)	$\epsilon_{sp}(p_f)$ (MeV)
0.21	0.682	−0.246	−0.194	0.016	−10.7	−20.8
0.22	0.658	−0.273	−0.215	0.013	−11.7	−21.7
0.23	0.634	−0.301	−0.238	0.008	−12.6	−22.4
0.24	0.609	−0.329	−0.260	0.003	−13.6	−22.5
0.25	0.584	−0.358	−0.285	−0.003	−14.4	−22.0
0.26	0.558	−0.388	−0.310	−0.009	−15.0	−20.4
0.27	0.531	−0.418	−0.337	−0.017	−15.5	−17.7
0.28	0.506	−0.444	−0.360	−0.018	−15.6	−13.4
0.29	0.479	−0.472	−0.386	−0.024	−15.2	−7.0
0.30	0.453	−0.502	−0.416	−0.032	−14.2	2.9
0.32	0.397	−0.562	−0.485	−0.048	−9.7	30.7
0.34	0.345	−0.615	−0.562	−0.061	−0.5	77.0
0.36	0.299	−0.662	−0.647	−0.068	14.7	143.4

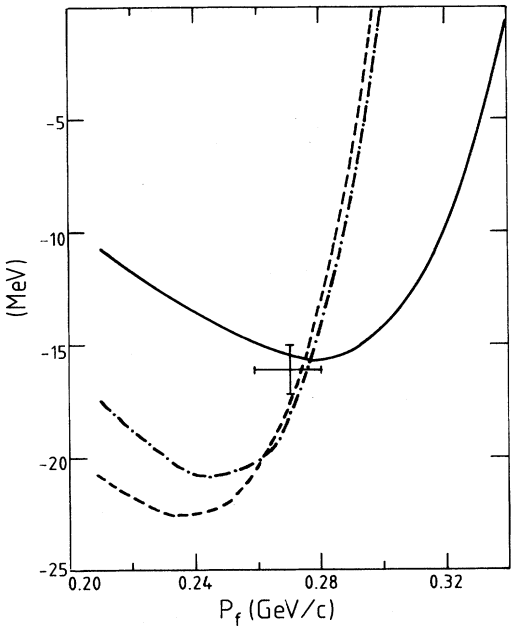

FIG. 2. The binding energy (full line), single-particle energy calculated by the definition Eq. (25) (dashed line), and the single-particle energy calculated by use of the Hugenholtz–van Hove theorem Eq. (36) (dash-dotted line). The cross indicates the empirical saturation point.

increased to about 0.275 GeV/c. This gives a saturation point that is well in agreement with the empirical values ($E_{\rm sat} = -16 \pm 1$ MeV, $p_{f_{\rm sat}} = 0.27 \pm 0.01$ GeV/c). At Fermi momenta around 0.20 GeV/c the binding energy is increased by ~ 1 MeV, at high densities the shift is small. The values of the self-consistent mass are shifted some 10 MeV downwards.

As stated before, the T-matrix approximation is a conserving approximation. An important property in many-body theory is the relation between single-particle energy [as defined in Eq. (25)] at the Fermi surface and the binding energy as expressed by the Hugenholtz–van Hove theorem [28], which is fulfilled by a conserving approximation:

$$\epsilon_{\rm sp}(p_f) = E_b + \frac{P}{\rho}, \tag{36}$$

where P is the pressure of the system, by definition $P \equiv \rho^2\, \partial E_b/\partial\rho$. The theorem is one specific example of general thermodynamic relations, here relating the chemical potential to the derivative of the free energy with respect to particle number. A special case is that, at saturation, the single-particle energy evaluated at the Fermi surface should equal the binding energy in a conserving approach. The Dirac-Brueckner model (and any other conventional Brueckner Hartree-Fock calculation), being the first order in the hole-line expansion [3] of the T-matrix approximation, is not conserving since conserving approximations treat particles and holes symmetrically. The nonconserving character of the relativistic Dirac-Brueckner model is expressed by the Hugenholtz–van Hove theorem being violated at saturation. For the Dirac-Brueckner approach is amounts to some 4 MeV. Nonrelativistic Brueckner calculations, however, give a typical violation of 15 MeV [3], so the Dirac-Brueckner model seems to be more conserving than its nonrelativistic counterpart. This is in agreement with calculations of Landau parameters: Relativistic approaches [29] do not violate the stability condition for F_0 whereas nonrelativistic calculations do violate this criterium.

Calculating the full T-matrix approximation, i.e., going to all orders in the hole-line expansion, the resulting equation-of-state and single-particle spectrum should fulfill the Hugenholtz–van Hove theorem since the approximation is conserving. Because the violation of the Hugenholtz–van Hove theorem was relatively small for the Dirac-Brueckner model, one expects beforehand that the shifts in the self-energies and binding energy will be small. Indeed this is the case, as we mentioned before. Also the Hugenholtz–van Hove theorem provides us with a check on the validity of the additional approximations we made when calculating the properties of the system. In the present calculation we find a violation of less than 0.5 MeV in the density region around saturation; see Fig. 2. This is within the numerical accuracy of our calculation. The violation increases with increasing pressure; this can only partly be ascribed to the problems associated with taking a numerical derivative. The pressure we calculate is systematically too low (in absolute sense) compared to the value needed to fulfill the Hugenholtz–van Hove theorem. This could be the consequence of the quasiparticle approximation and the neglect of the momentum dependence of the self-energy. Our results concerning the Hugenholtz–van Hove theorem are comparable with the results of Baldo *et al.* [13], although these authors only give a value at saturation density and only go to second order in the hole-line expansion. Other calculations including hole-hole propagation [14, 30] do not give explicit results on the fulfillment of the Hugenholtz–van Hove theorem. We think these are very desirable since the theorem is an easy though powerful check on the consistency of a particular approach.

The compression modulus of nuclear matter is defined by

$$K = 9\frac{\partial}{\partial\rho}\left(\rho^2\frac{\partial}{\partial\rho}E_b\right) = 4p_f\frac{\partial}{\partial p_f}E_b + p_f^2\frac{\partial^2}{\partial p_f^2}E_b. \tag{37}$$

The empirical value at saturation is commonly assumed to be 210 ± 30 MeV [31]; the most recent value based on the giant monopole resonance is 300 ± 25 MeV [32]. A compilation of different methods of extracting the compressibility from available data favors a value of around 300 MeV [33]. However, there are some doubts about how to extrapolate the experimental values for finite nuclei to infinite nuclear matter [34]. The Dirac-Brueckner model gives a compression modulus of 250 MeV [9], the same as quoted by Machleidt [35]. Nonrelativistic models tend to give lower values, e.g., Machleidt gives 180 MeV for the nonrelativistic equivalent of

his model. In the present calculation we find 310 MeV, i.e., an increase of 60 MeV as compared to the Dirac-Brueckner results. The value is compatible with the value given by Glendenning [33]. A closer examination shows that the compression modulus rapidly increases around the saturation point. This is the case both for our calculation and the Dirac-Brueckner model. Also the relativistic calculation of Machleidt shows this behavior, whereas his nonrelativistic calculation appears to have a much less rapid increase. The effect illustrated in Fig. 3. The comparison is somewhat obscured by the totally different saturation points but the different behavior is obvious. This effect strongly reduces the validity of the compression modulus as an expansion parameter of the equation of state around saturation. Also we observe a more rapid increase of the compressibility than found by using the estimate of the relativistic effect on the binding energy [35, 36], $\Delta E_{\rm rel} \approx (2\ {\rm MeV})(\rho/\rho_0)^{8/3}$.

The inclusion of hole-hole propagation also allows us to perform a sensible calculation of the relativistic mean field for momenta below the Fermi momentum. As before [9] we define the relativistic mean-field by

$$\begin{aligned} {\rm Re}[U(p)] &= E_p^* - {\rm Re}[\Sigma_0^{(+)}(p)] - E_p, \\ {\rm Im}[U(p)] &= {\rm Im}\left(\frac{m^*}{E_p^*}\Sigma_s^{(+)} - \Sigma_0^{(+)} + \frac{p^*}{E_p^*}p\,\Sigma_v^{(+)}\right), \end{aligned} \tag{38}$$

where we now explicitly include the momentum dependence of the self-energies. The incoming momentum p appearing in Σ^+ is taken on-shell according to the condition

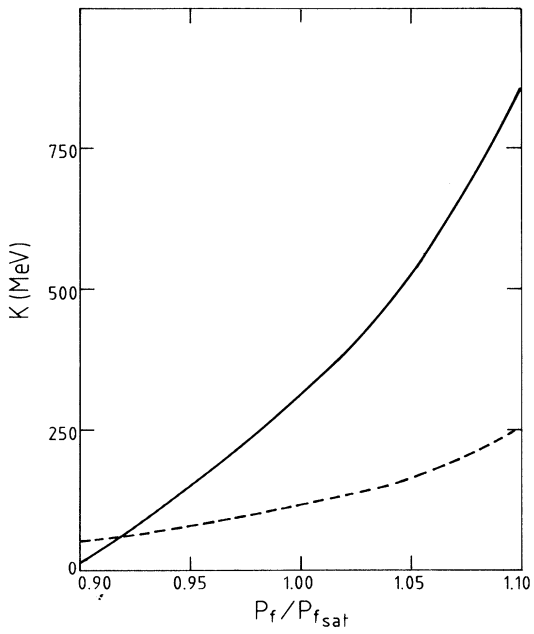

FIG. 3. The compressibility around saturation. Values are given for the relative Fermi momentum around saturation $p_f/p_{f_{\rm sat}}$. The full line is our result, the dashed line is calculated from the nonrelativistic values of Machleidt [35].

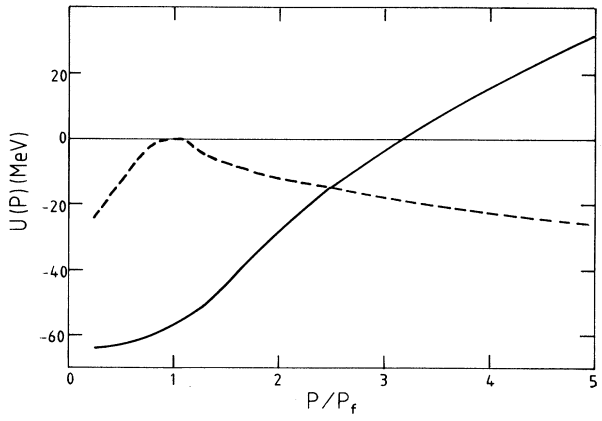

FIG. 4. The relativistic mean field Eq. (38) at Fermi momentum 0.27 GeV/c as a function of the relative momentum p/p_f. The full line is the real part, the dashed line the imaginary part.

$$p_0 = (\bar{p}^2 + m_{\rm sc}^*)^{\frac{1}{2}} - \Sigma_{0,{\rm sc}}^{(+)}. \tag{39}$$

The subscript sc refers to the fact that we have to use here the self-consistent values at the Fermi surface. Results of this calculation are given in Table III and presented in Fig. 4, taking for the Fermi momentum $p_f = 0.27$ GeV/c. As in the nonrelativistic calculation of Baldo *et al.* [13] we observe a "flattening" of the mean-field in the Fermi sea. The value of the mean field at the Fermi surface is −57 MeV. At higher energies the behavior is very much the same as in the Dirac-Brueckner case, it crosses zero at around 300 MeV, and it shows a characteristic flattening behavior at higher momenta. These characteristics are also present in the empirical Woods-Saxon depths [37], the variational calculations of $U(\rho, k)$ of Wiringa [38], and the realistic parametrizations of the single-particle potential used by Gale *et al.* [39].

TABLE III. The relativistic mean field at $p_f = 0.27$ GeV/c. Re(U) and Im(U) are calculated as prescribed by Eq. (38).

p/p_f	Re(U) (MeV)	Im(U) (MeV)
0.25	−65	−24.0
0.5	−63	−13.5
0.75	−60	−3.0
1.0	−57	0.0
1.25	−52	−3.5
1.5	−44	−7.5
2.0	−28	−12.0
3.0	−4	−17.0
4.0	16	−22.5
5.0	32	−26.0

B. Spectral function and occupation probabilities

By making the quasiparticle approximation one ignores the energy dependence (p_0) of the self-energy and sets the imaginary part to zero for all incoming energies. This approximation greatly simplifies the calculations, since the p_0 integrations can be carried out explicitly. Going beyond this and taking the full energy dependence of the self-energy into account in the self-consistent solution of Eq. (12) is beyond our present computational capabilities. The formalism itself, however, is clear about how to deal with this. As a first step towards a fully self-consistent solution we calculate the energy depence of the self-energy in the quasiparticle approximation, and with this we calculate the spectral function. We still ignore the imaginary part of the self-energy in the solution of Eq. (12). With the spectral function we can calculate the momentum distribution (occupation probabilities) of the particles.

In the Brueckner models the imaginary part of the self-energy is zero below the Fermi energy, and the spectral is a δ function of the energy p_0. Consequently, the Fermi sea consists of quasiparticles in these models. Upon inclusion of hole-hole intermediate states, the self-energy obtains an imaginary part below the Fermi energy. So in our model the spectral function of particles in the Fermi sea is not a δ function but has a width induced by the imaginary part of the self-energy.

From now on we will again use the definitions of Eq. (15) for the effective quantities. The particular expressions of the contributions to $\Sigma^{(+)}$ are easily extended to the case of arbitrary incoming $(p_0, \bar{p})$. The T matrices needed in the evaluation of $\Sigma^{(+)}$ are still calculated using the self-consistent mass determined at the Fermi surface. We calculate the self-energies as a function of p_0^* rather than of p_0, so we have to transform the integration in Eq. (22) to become

$$\int_{-\infty}^{\infty} \frac{dp_0^*}{2\pi} \left(1 - \frac{\partial \Sigma_0^{(+)}}{\partial p_0^*}\right) \tilde{a}(p_0^*, \bar{p}) = 1. \tag{40}$$

For a given momentum $\bar{p}$ we calculate for a grid of energies the Lorentz components of the self-energies. We then form the parts $\mathrm{Im}(\Sigma_0^{(+)} - \Sigma_s^{(+)} m^*/E_p^* - p\Sigma_v^{(+)} p^*/E_p^*)$ and $p_0^* - E_p^*$. These are interpolated with splines. By putting this spline interpolation into Eq.(21) we can calculate the spectral function $\tilde{a}(p_0^*, \bar{p})$ for any required p_0. As can be seen from Fig. 5 the spectral function looks very much like its nonrelativistic counterpart [14]. With this interpolation we can locate the zero of $p_0^* - E_p^*$ as a function of p_0. This defines the position of the quasiparticle peak of the spectral function, $p_{0,\mathrm{qp}}$. We regularize the integration over the spectral function by subtracting a suitable function so that the behavior around the quasiparticle peak is smoothed. The integration over the subtracted function can be carried out analytically. We have performed a calculation for a range of momenta $\bar{p}$ at a Fermi momentum $p_f = 0.27$ GeV/c. The sum rule Eq. (40) is satisfied within a margin of 3%. Only in the neighborhood of the Fermi momentum $[(0.95\text{–}1.05)p_f]$ are the discrepancies higher. This is caused by the fact that the imaginary part vanishes at $p_0 = \epsilon^*(p_f)$. When the quasiparticle peak is close to $\epsilon^*_{p_f}$ the error in the imaginary part becomes dominant. This all is mainly the consequence of decomposing the self-energy in Lorentz components, an additional step not present in nonrelativistic calculations (see, e.g., Ramos *et al.* [14]).

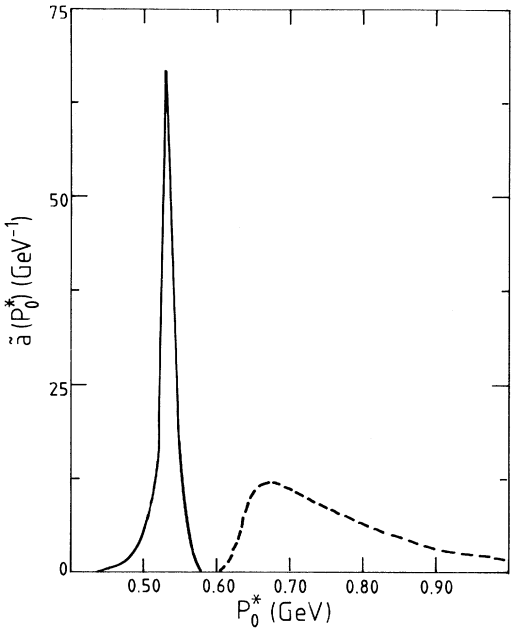

FIG. 5. The spectral function $\tilde{a}(p)$, Eq. (23), for $p = 0.75 p_f$ ($p_f = 0.27$ GeV/c), as a function of the effective incoming energy p_0^*. The values above the Fermi energy (dashed line) were multiplied by 10.

With the spectral function we can find the occupation probability

$$n(\bar{p}) = \int_{-\infty}^{\epsilon^*_{\mathrm{up}}} \frac{dp_0^*}{2\pi} \left(1 - \frac{\partial \Sigma_0^{(+)}}{\partial p_0^*}\right) \tilde{a}(p_0^*, \bar{p}), \tag{41}$$

where the upper limit of the integration $\epsilon^*_{\mathrm{up}} = \epsilon^*_{\mathrm{sp}}(p_f) + \Sigma_0^{(+)}$. Because of the number conservation the occupation probabilities should obey the sum rule

$$\frac{1}{\rho} \int d\bar{p}\, n(\bar{p}) = 1. \tag{42}$$

The results for the occupation probabilities are presented in Fig. 6 and Table IV. Compared with the results of Jaminon and Mahaux [16] we find a significantly lower $n(p)$ for momenta below the Fermi momentum. These authors used a parametrization of the Dirac-Brueckner results for the mean field above the Fermi sea. By taking phase-space arguments and the sum rule in Eq. (42) into account they were able to estimate the occupation probabilities in the Dirac-Brueckner model up to second order in the hole-line expansion. The average depletion of the Fermi sea is defined by

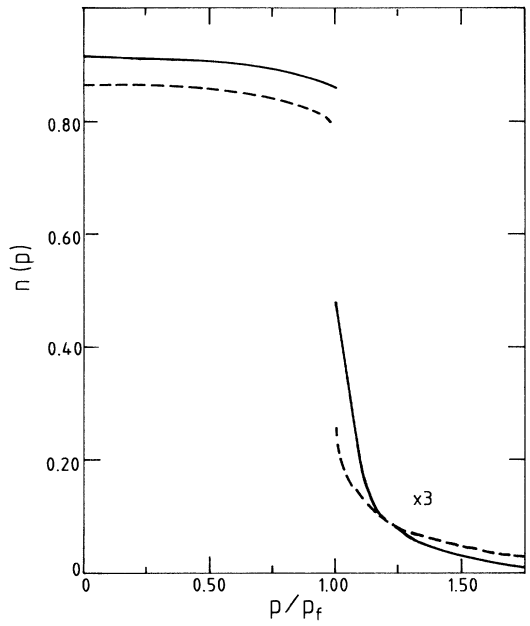

FIG. 6. The occupation probabilities at the Fermi momentum 0.27 GeV/c (full line); for reference the variational results of Fantoni and Pandharipande [2] (dashed line) also are given. Both curves were multiplied by a factor of 3 for values $p > p_f$.

$$\kappa = 1 - \frac{1}{\rho}\int_0^{p_f} d\bar{p}\, n(\bar{p}). \tag{43}$$

Jaminon and Mahaux find a value about 5%. We obtain a much higher value of 11%. From this one might conclude that the higher-order terms in the hole-line expansion give an essential contribution to the depletion of the Fermi sea. Also, we note that the particle number sum rule Eq. (42) is fulfilled very well within the numerical accuracy.

TABLE IV. The occupation probabilities for $p_f = 0.27$ GeV/c.

p/p_f	$n(p)$
0.25	0.91
0.50	0.905
0.75	0.895
0.875	0.88
0.95	0.87
1.0^-	0.86
1.0^+	0.16
1.05	0.10
1.125	0.05
1.25	0.027
1.50	0.01
2.0	0.003

The discontinuity of $n(p)$ at the Fermi momentum is equal to the quasiparticle strength at the Fermi surface. In our case we obtain for this quantity

$$Z(p_f) = \left[\frac{\partial}{\partial p_0}(p_0^* - E_p^*)\right]^{-1}, \tag{44}$$

where the derivatives are taken at the Fermi energy $p_0^* = \epsilon_{p_f}^*$. We calculate a value of around 0.7. Extrapolating $n(p)$ from below towards p_f gives $n(p_f^-) \approx 0.86$. The limit $p \downarrow p_f$ is more ambiguous, $n(p)$ is very steep slightly above the Fermi momentum. Taking $n(p_f^+) \approx 0.16$ is compatible with the previous values and the values of $n(p)$ we calculated above the Fermi surface. These uncertainties do not affect the average depletion κ, since only a small region is affected.

Also we calculated the moments of the kinetic energy and p_0 of the spectral function

$$\langle V\rangle = \frac{1}{\rho}\int d\bar{p}\int_{-\infty}^{\epsilon_{\rm up}^*}\frac{dp_0^*}{2\pi}\left(1 - \frac{\partial\Sigma_0^{(+)}}{\partial p_0^*}\right) p_0\,\tilde{a}(p_0^*,\bar{p}) - m_N,$$
$$\langle K\rangle = \frac{1}{\rho}\int d\bar{p}\,(E_p - m_N)\,n(\bar{p}), \tag{45}$$

with $n(\bar{p})$ defined in Eq. (41) and $\epsilon_{\rm up}^*$ defined above. The sum $\frac{1}{2}(\langle V\rangle + \langle K\rangle)$ is, by definition [18], the energy of the system. For $\langle V\rangle$ we find a value around -53 MeV; for the kinetic energy we find 27.5 MeV. So the binding energy calculated with the spectral function is ~ -13 MeV. This is in quite good agreement with the binding energy calculated in the quasiparticle approximation. There we obtained -15.5 MeV.

The empirical values of κ and $Z(p_f)$ are not very well established yet. Much effort is put into this at the present moment by means of (e,e',p) experiments [40]. The values are difficult to evaluate due to finiteness and surface effects. Mahaux [41] cites a value of $\kappa = 0.15 \pm 0.05$, from (e,e',p) experiments one could deduce $Z(p_f) = 0.50 \pm 0.05$ [40]. This is to be compared with our calculated values, $Z(p_f) = 0.7$ and $\kappa = 0.11$. These two quantities are somewhat related: A high κ will be accompanied by a low $Z(p_f)$ and vice versa. Also, note that the coupling-to-surface vibrations in finite nuclei can decrease Z with ~ 0.2 as compared to the value in nuclear matter [2].

Within a nonrelativistic framework many results on the occupation probabilities are available, e.g., the variational results of Fantoni and Pandharipande [2], Benhar *et al.* [15], the Brueckner results of Sartor *et al.* [12], Jeukenne *et al.* [3], Grange *et al.* [11], Baldo *et al.* [13], and the Green's-function approach of Ramos *et al.* [14] (which is, apart from the nonrelativistic character, the most akin to our approach). All these calculations come up with a depletion in the range 15–25 % and a $Z(p_f)$ of 0.5–0.7. This is compatible with the available data.

The nonrelativistic Brueckner results mentioned above

all are calculations up to second order in the hole-line expansion. So one might expect an increase in the depletion when going to all orders in the hole-line expansion in these calculations. The calculation of Ramos *et al.* [14] does go to all orders in the hole-line expansion. However, they use a truncated version of the Reid potential, so it is difficult to compare their results with previous mentioned Brueckner calculations in the same fashion as we could do with the calculations of Jaminon and Mahaux [16]. Since the details of the nucleon-nucleon interaction used do play a significant role in the magnitude of the depletion, especially the strength of the tensor force [2], the results of Ref. [14] have only a restricted applicability.

At present we do not have a physical explanation as to why we find a small depletion in our relativistic model. Again we want to stress that a small κ is consistent with the small violation of the Hugenholtz–van Hove theorem in the Dirac-Brueckner model. As we already pointed out, this implies a quick convergence of the hole-line expansion. The convergence is believed to be governed by κ, so the small κ we calculated is consistent with our previous results. Finally we want to note that Machleidt [35] gives for his relativistic calculation a value of the "wound integral" of 13% at saturation and a violation of the Hugenholtz–van Hove theorem of 5.5 MeV. In nonrelativistic Brueckner theory the "wound integral" should be of the same order as κ, this argument points to a κ compatible with our result. The small violation of the Hugenholtz–van Hove theorem also points to a κ of about the same size as we calculated. So it might be interesting to see whether the small depletion also persists when using other interactions which might have a different short-range behavior but also describe nuclear scattering data like, e.g., the Bonn interaction.

IV. SUMMARY

We presented a calculation of the equilibrium properties of nuclear matter based on a "conserving" relativistic many-body theory. This meant that we incorporated all orders of the hole-line expansion into our calculation. For the equation of state we found a small shift towards the empirical saturation point. In fact, the saturation point we find is within the error bars of the empirical saturation point. Also, we found a higher value of the compressibility, 310 MeV, which is still compatible with the empirical values [33]. We checked on the conserving character of our approach by testing the fullfillment of the Hugenholtz–van Hove theorem. The violation was found to be practically zero around saturation. Farther away from saturation the discrepancy was calculated to be a few MeV.

We calculated the relativistic mean field and found this to have the same characteristics as in the Dirac-Brueckner model. Also we found a "flattening" of the mean field within the Fermi sea. This is also present in nonrelativistic calculations which include higher orders of the hole-line expansion [13].

We argued that the small violation of the Hugenholtz–van Hove theorem already observed in the Dirac-Brueckner model pointed towards a small value of the depletion of the Fermi sea κ, since this parameter governs the convergence of the hole-line expansion. A small κ is also consistent with the small shift in the saturation properties. In an actual calculation of the occupation probabilities by means of a spectral function we found $\kappa \sim 0.11$. This is small when compared with nonrelativistic Brueckner calculations although it is higher than the estimate of Jaminon and Mahaux based on our previous Dirac-Brueckner results. The discontinuity at the Fermi momentum of the occupation probabilities, equal to the quasiparticle strength at the Fermi surface, was found to be 0.7.

As a check we calculated the binding energy by one of its (formally) equivalent definitions and found this to be compatible with the value calculated within the quasiparticle approximation. This, together with the reproduction of the empirical saturation point and the fulfillment of the Hugenholtz–van Hove theorem around saturation, leads to the conclusion that the equation of state as we calculated in the quasiparticle approximation provides a good description of nuclear matter around saturation.

The authors acknowledge stimulating discussions with Dr. L. Dieperink and Dr. B. Friman.

[1] B.D. Serot and J.D. Walecka, in *Advances in Nuclear Physics*, edited by J.W. Negele and E. Vogt (Plenum, New York, 1986), Vol. 16, p. 1.
[2] S. Fantoni and V.R. Pandharipande, Nucl. Phys. **A427**, 473 (1984).
[3] J.P. Jeukenne, A. Lejeune, and C. Mahaux, Phys. Rep. **25**, 83 (1976).
[4] R. Machleidt, K. Holinde, and Ch. Elster, Phys. Rep. **149**, 1 (1987).
[5] C. Mahaux and R. Sartor, Phys. Rev. C **19**, 229 (1979).
[6] F. Coester, S. Cohen, B. Day, and C.M. Vincent, Phys. Rev. C **1**, 769 (1970).
[7] B.D. Day, Phys. Rev. Lett **47**, 226 (1981); B.D. Day and R.B. Wiringa, Phys. Rev. C **32**, 1057 (1985).
[8] L.S. Celenza and C.M. Shakin, *Relativistic Nuclear Physics* (World Scientific, Singapore, 1986).
[9] B. ter Haar and R. Malfliet, Phys. Rep. **149**, 207 (1987); R. Malfliet, in *Progress in Particle and Nuclear Physics*, edited by A. Faessler (1988), Vol. 21, p. 207; B. ter Haar and R. Malfliet, Phys. Rev. Lett. **59**, 1652 (1987).
[10] C.J. Horowitz and B.D. Serot, Nucl. Phys. **A464**, 613 (1987).
[11] P. Grange, J. Cugnon, and A. Lejeune, Nucl. Phys. **A473** 365 (1987).
[12] R. Sartor and C. Mahaux, Phys. Rev. C **21**, 1546 (1980).
[13] M. Baldo, F. Bombaci, G. Giansiracusa, U. Lombardo, C. Mahaux, and R. Sartor, Phys. Rev. C **41**, 1748 (1990).
[14] A. Ramos, A. Polls, and W.H. Dickhoff, Nucl. Phys. **A503**, 1 (1990).
[15] O. Benhar, A. Fabrocini, and S. Fantoni, Phys. Rev. C **41**, R24 (1990).
[16] M. Jaminon and C. Mahaux, Phys. Rev. C **41**, 697

(1990).
[17] G. Baym and L.P. Kadanoff, Phys. Rev. **124**, 287 (1961).
[18] W. Botermans and R. Malfliet, Phys. Rep. **198**, 115 (1990).
[19] L.V. Keldysh, Zh. Eksp. Teor. Fiz. **42**, 1515 (1964) [Sov. Phys. JETP **20**, 1018 (1965)].
[20] John W. Negele and Henri Orland, *Quantum Many Particle Systems* (Addison-Wesley, Redwood City, 1988).
[21] S.S. Schweber, *An Introduction to Relativistic Quantum Field Theory* (Harper and Row, New York, 1961).
[22] P. Poschenrieder and M.K. Weigel, Phys. Rev. C **38**, 471 (1988).
[23] P. Nozières, *Theory of Interacting Fermi Systems* (Benjamin, New York, 1964).
[24] H. Elsenhans, H. Müther, and R. Machleidt, Nucl. Phys. **A515**, 715 (1990).
[25] T. Cheon and E.F. Redish, Phys. Rev. C **39**, 331 (1989).
[26] J.A. Tjon and S.J. Wallace, Phys. Rev. C **35**, 280 (1987).
[27] F. de Jong and R. Malfliet, KVI Annual Report 1989, p. 78.
[28] N.M. Hugenholtz and L. van Hove, Physica **23**, 525 (1958).
[29] K. Nakayama, S. Drozdz, S. Krewald, and J. Speth, Nucl. Phys. **A470**, 573 (1987).
[30] M.F. Jiang, T.T.S. Kuo, and H. Müther, Phys. Rev. C **38**, 2408 (1988); **40**, 1836 (1989).
[31] J.D. Blaizot, D. Gogny, and B. Grammaticos, Nucl. Phys. **A265**, 315 (1976).
[32] M.M. Sharma, W.T.A. Borghols, S. Brandenburg, S. Crona, A v.d. Woude, and M.N. Harakeh, Phys. Rev. C **38**, 2562 (1988).
[33] N.K. Glendenning, Phys. Rev. C **37**, 2733 (1988).
[34] G.E. Brown, Nucl. Phys. **A488**, 689c (1988).
[35] R. Machleidt, in *Advances in Nuclear Physics*, edited by J.W. Negele and E. Vogt (Plenum, New York, 1989), Vol. 19, p. 189.
[36] G.E. Brown, W. Weise, G. Baym, and J. Speth, Comments Nucl. Part. Phys. **17**, 39 (1987).
[37] B. Friedman and V.R. Pandharipande, Phys. Lett. B **100**, 205 (1981).
[38] R.B. Wiringa, Phys. Rev. C **38**, 2967 (1988).
[39] C. Gale, G.M. Welke, M. Prakash, S.J. Lee, and S. Das Gupta, Phys. Rev. C **41**, 1545 (1990).
[40] L. Lapikás, in Proceedings of the Sixth Mini-Conference on Electron Scattering: Past and Future, Amsterdam, 1989 (unpublished).
[41] C. Mahaux, in *Nuclear Matter and Heavy Ion Collisions*, edited by M. Soyeur, H. Flocard, B. Tamain, and M. Porneuf (Plenum, New York, 1989).